Spectrochimica Acta Part A: Molecular and Biomolecular Spectroscopy 124 (2014) 21–29

Contents lists available at ScienceDirect

Spectrochimica Acta Part A: Molecular and Biomolecular Spectroscopy

journal homepage: www.elsevier.com/locate/saa

Dinuclear nickel(II) triple-stranded supramolecular cylinders: Syntheses, characterization and G-quadruplexes binding properties

Xin-Xin Xu [a], Jing-Jing Na [a], Fei-Fei Bao [a], Wen Zhou [a], Chun-Yan Pang [a], Zaijun Li [a], Zhi-Guo Gu [a,b,*]

[a] School of Chemical and Material Engineering, Jiangnan University, Wuxi 214122, PR China
[b] The Key Laboratory of Food Colloids and Biotechnology, Ministry of Education, School of Chemical and Material Engineering, Jiangnan University, Wuxi 214122, PR China

HIGHLIGHTS

- Three dinuclear nickel triple-stranded supramolecular cylinders were synthesized.
- The cylinders could bind to G-quadruplexes with high binding constants.
- **1** could convert G-quadruplexes from antiparallel to hybrid structure in Na^+ solution.

GRAPHICAL ABSTRACT

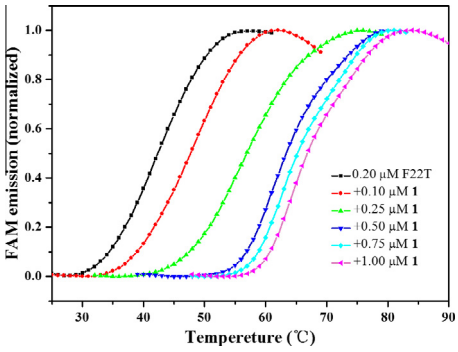

ARTICLE INFO

Article history:
Received 3 November 2013
Received in revised form 10 December 2013
Accepted 23 December 2013
Available online 7 January 2014

Keywords:
Dinuclear
Supramolecular cylinders
Schiff base
G-quadruplex
DNA binding
Stabilizers

ABSTRACT

Three dinuclear nickel triple-stranded supramolecular cylinders $[Ni_2(L1)_3][ClO_4]_4$ (**1**), $[Ni_2(L2)_3][ClO_4]_4$ (**2**) and $[Ni_2(L3)_3][ClO_4]_4$ (**3**) with bis(pyridylimine) Schiff base containing triphenyl groups in the spacers as ligands were synthesized and characterized. The human telomeric G-quadruplexes binding properties of cylinders **1**–**3** were evaluated by means of UV–Vis spectroscopy, circular dichroism (CD) spectroscopy and fluorescence resonance energy transfer (FRET) melting assay. UV–Vis studies revealed that the supramolecular cylinders **1**–**3** could bind to G-quadruplex DNA with high binding constants (K_b values ranging from 0.11–2.2 × 10^6 M^{-1}). FRET melting studies indicated that the cylinders **1**–**3** had much stronger stabilizing effect on G-quadruplex DNA (ΔT_m up to 24.5 °C) than the traditional cylinder $Ni_2L_3^{4+}$ just containing diphenylmethane spacers (ΔT_m = 10.6 °C). Meanwhile, cylinders **1**–**3** were found to have a modest degree of selectivity for the quadruplex DNA versus duplex DNA in competition FRET assays. Moreover, CD spectroscopy revealed that complex **1** could induce G-quadruplex formation in the absence of metal ions solution and convert antiparallel G-quadruplex into hybrid structure in Na^+ solution. These results provided a new insight into the development of supramolecular cylinders as potential anticancer drugs targeting G-quadruplex DNA.

Introduction

G-quadruplex DNA has attracted much interest in several research fields including chemistry, biology and pharmacology over the past decades [1]. G-quadruplex DNA sequences have an unusual structure formed from stacks of four in plane guanine bases in a circle through hoogsteen hydrogen-bonding interactions [2]. Alkali metal cations (such as Na^+ and K^+) can further stabilize secondary structures of G-quadruplex DNA via engaging in electrostatic interactions with the guanine carbonyl groups [3]. Folding telomeric DNA into four-stranded G-quadruplexes can inhibit telomerase elongation of telomeres by interrupting the interaction between the enzyme and single-stranded telomeric DNA substrate

* Corresponding author at: School of Chemical and Material Engineering, Jiangnan University, Wuxi 214122, PR China. Tel.: +86 510 85917090; fax: +86 510 85917763.
E-mail address: zhiguogu@jiangnan.edu.cn (Z.-G. Gu).

1386-1425/$ - see front matter © 2014 Elsevier B.V. All rights reserved.
http://dx.doi.org/10.1016/j.saa.2013.12.102

[4]. Telomere quadruplexes are potential tumor-selective drug targets for cancer chemotherapy and modulation of gene transcription [5]. Therefore, G-quadruplexes stabilizing compounds have become an attractive platform for designing anticancer drugs [6].

Molecules can interact with the G-quadruplexes by face, edge, loop or groove recognition through stacking, H-bonding, and electrostatic interactions. The weak non-covalent interactions are very important in controlling the structure and are vital for molecular recognition of G-quadruplex DNA [7]. The majority of quadruplex DNA binders reported to date based on organic molecules with large planar π-aromatic surface could stack on the quadruplex [8]. Some metal complexes with hetero aromatic multidentate ligands have been proved to be excellent stabilizers of quadruplex DNA [9]. For example, functionalized nickel(II) salphen complexes with cationic side arms displayed a high degree of G-quadruplexes stabilization (at best ΔT_m = 33.8 °C) and considerable selectivity (50-fold) for G-quadruplex DNA versus duplex DNA [10]. Recently supramolecular complexes have emerged as a new and very exciting class of quadruplex DNA stabilizers [11]. Qu and co-workers reported that tetracationic chiral bimetallic cylinders $[M_2L_3]^{4+}$ (M = Fe^{II}, Ni^{II}) based on bis(pyridylimine) ligand (Scheme 1a), whose shapes were comparable with the recognition surface of zinc finger protein, were shown to interact with quadruplex DNA and to exhibit good antitumor activities [12,13]. Only *P*-enantiomer of $[M_2L_3]^{4+}$ had the ability to convert antiparallel G-quadruplex into a hybrid form in the presence of sodium and to selectively induce G-quadruplex formation under salt-deficient conditions [12,13]. However, to the best of our knowledge, no other bimetallic cylinder based on diimine ditopic ligands except for $[M_2L_3]^{4+}$ systems has been reported as G-quadruplex stabilizers.

In this paper, three new bis(pyridylimine) Schiff base ligands (Scheme 1b) containing triphenyl groups in the spacers (L1–L3) instead of L have been used to construct novel dinuclear nickel(II) supramolecular cylinders $[Ni_2(L1)_3][ClO_4]_4$ (**1**), $[Ni_2(L2)_3][ClO_4]_4$ (**2**) and $[Ni_2(L3)_3][ClO_4]_4$ (**3**) and analyze the influence of this substitution on G-quadruplex DNA binding abilities. As we know, nickel is an essential element in many biological processes [14], and many new nickel(II) complexes have been researched for potential applications in various fields [15]. Meanwhile, the four positive charges of the cylinders will significantly contribute to the strength of the electrostatic interactions of such species to the anionic DNA [16]. More importantly, the introduction of the additional aromatic rings in the spacers can increase the size of the cylinders which is possible to enhance the non-covalent interactions between the synthetic supramolecular cylinders and G-quadruplexes. UV–Vis spectroscopy, CD spectroscopy and FRET melting assay were used to assess the human telomeric G-quadruplex DNA binding properties of the cylinders **1–3**. The experimental results have shown that the structure characters of the cylinders played an important role in the stabilizing ability of G-quadruplexes.

Experimental

Materials and methods

DNA oligomers or primers, 5′-AG3(T2AG3)-3′ (HTG22), double stranded competitor 5′-CAATCGGATCGAATTCGATCCGATTG-3′ (ds26), 5′-FAM-AG3(T2AG3)-TAMRA-3′ (F22T) (FAM = 6-carboxyfluorescein, TAMRA = 6-carboxytetrame-thylrhodamine), were synthesized by Sangon Biotechnology (Shanghai, China) and were used without further purification. Calf thymus DNA (ct-DNA) was purchased from Sigma–Aldrich (Shanghai, China) Co. Ltd. Concentrations of HTG22 and F22T were determined by measuring the absorbance at 260 nm after melting. Single-strand extinction coefficients were calculated from mononucleotide data using a nearest-neighbor approximation [17]. The formations of intramolecular G-quadruplexes were carried out as follows: the oligonucleotide samples, dissolved in different buffers (buffer A: 10 mM tris(hydroxymethyl)methanamin-HCl (Tris–HCl), pH = 7.4; buffer B: 100 mM NaCl, 10 mM Tris–HCl, pH = 7.4; buffer C: 100 mM KCl, 10 mM Tris–HCl, pH = 7.4.), were heated to 95 °C for 5 min, gently cooled to room temperature and then incubated at 4 °C overnight. The solution of ct-DNA was prepared in buffer D (50 mM NaCl, 5 mM Tris–HCl, pH = 7.2), and gave the ratio of UV absorbance at 260 and 280 nm, A_{260}/A_{280} = 1.9, indicating that the ct-DNA was sufficiently free of protein [18]. The ct-DNA concentration (moles of bases per liter) was determined spectroscopically by using the molar extinction coefficient: ε_{260} = 6600 cm^{-1} mol^{-1} · dm^3. All stock solutions were stored at 4 °C and used after no more than 4 days. All other reagents and solvents were purchased from commercial sources and used without further purification. Ultrapure water (18.2 MΩ cm) was used in all experiments. Concentrations of stock solutions of the metal complexes were 1 mM in acetonitrile. Further dilution was made in the corresponding buffer according to the required concentrations for all the experiments. All other reagents employed were of analytical reagent grade or with highest quality and were purchased from commercial sources and used without further purification.

^{1}H NMR spectra ware recorded on AVANCE III (400 MHz) instrument at 298 K using standard Bruker software. The spectra were

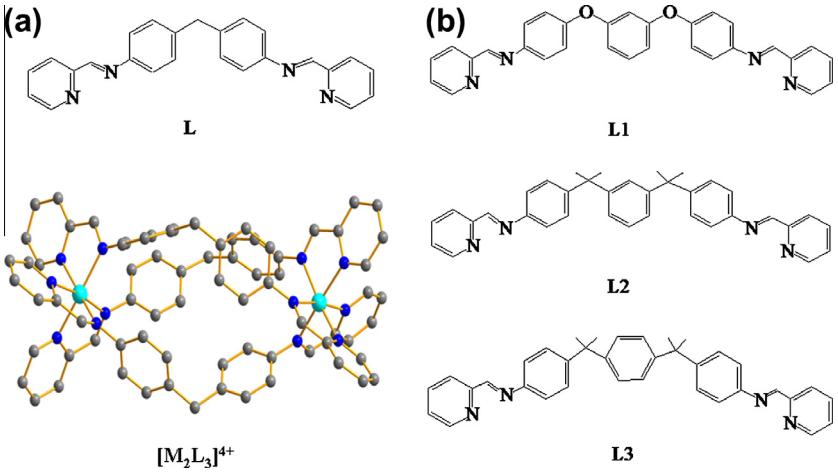

Scheme 1. (a) Schematic drawing of ligand L and triple-stranded cylinder cations $[M_2L_3]^{4+}$ (M = Fe^{II}, Ni^{II}). (b) Schematic drawing of the ligands L1–L3.

internally referenced using the residual protio solvent resonance relative to tetramethylsilane (δ = 0 ppm). The electrospray ionization mass spectrometry (ESI-MS) spectra were recorded using an LCQ fleet APT/SSQ-710 ESI-MS spectrometer (Finnigan MAT). Infrared spectra were measured on an ABB Bomem FTLA 2000-104 spectrometer with KBr pellets in the 400–4000 cm^{-1} region. Element analyses were conducted on elementar corporation vario EL III analyzer. UV–Vis absorbance spectra were collected on Shimadzu UV-2101 PC scanning spectrophotometer.

Synthesis

Synthesis of L1

A solution of 2-pyridinecarboxaldehyde (0.512 g, 4.8 mmol) in acetonitrile (15 mL) was added dropwise to a solution of 1,3-bis(4-aminophenoxy)benzene (0.702 g, 2.4 mmol) in 15 mL acetonitrile at room temperature. The reaction mixture was heated at reflux for 3 h. After the reaction was completed, the solvent was removed under reduced pressure to get the crude ligand, which was washed with ethanol several times and dried in vacuo to get L1 as yellow powder in sufficient high purity. Yield, 76%. ^{1}H NMR (400 MHz, $CDCl_3$ δ ppm): 8.715 (d, J = 4.4 Hz, 2H, H^2), 8.630 (s, 2H, H—C═N), 8.207–8.188 (d, J = 7.6 Hz, 2H, H^5), 7.810 (t, 2H, H^4), 7.367–7.338 (m, 2H, H^3), 7.338–7.264 (m, 5H, $H^{a,e}$), 7.083 (d, J = 12.4 Hz, 4H, H^b), 6.786–6.765 (d, 3H, $H^{c,d}$); IR (KBr cm^{-1}): v = 3051 (w), 2916 (w), 2850 (w), 1631 (m), 1581 (s), 1498 (vs), 1479 (vs), 1347 (w), 1269 (w), 1228 (vs), 1126 (w), 962 (w), 881 (w), 837 (m), 775 (m); Anal. Calcd (%) for $C_{30}N_4H_{22}O_2$: C 76.58, H 4.71, N 11.91, Found: C 76.63, H 4.65, N 11.84.

Synthesis of L2

The ligand L2 was prepared from 1,3-bis[1-(4-aminophenyl)-1-methylethyl]benzene (0.826 g, 2.4 mmol) and 2-pyridinecarboxaldehyde (0.512 g, 4.8 mmol) by the method described above for L1, and was obtained as light yellow oil. Yield, (70%). ^{1}H NMR (400 MHz, $CDCl_3$ δ ppm): 8.702 (d, J = 4.4 Hz, 2H, H^2) 8.640 (s, 2H, H—C═N), 8.202 (d, J = 8.0 Hz, 2H, H^5), 7.792 (t, 2H, H^4), 7.356 (t, 2H, H^3), 7.283–7.216 (m, 9H, $H^{a,b,d}$), 7.147 (s, 1H, H^c), 7.116–7.097 (t, 2H, H^e), 1.683 (s, 12H, CH_3); IR (KBr cm^{-1}): v = 3057 (w), 2968 (s), 2870 (w), 1628 (w), 1583 (m), 1566 (w), 1500 (vs), 1465 (s), 1435 (m), 1361 (w), 1205 (w), 1178 (w), 993 (w), 883 (w), 833(s), 775 (m); Anal. Calcd (%) for $C_{36}N_4H_{34}$: C 82.72, H 6.56, N 10.72, Found: C 82.77, H 6.49, N 10.68.

Synthesis of L3

The ligand L3 was prepared from 1,4-bis[1-(4-aminophenyl)-1-methylethyl]benzene (0.826 g, 2.4 mmol) and 2-pyridinecarboxaldehyde (0.512 g, 4.8 mmol) by the method described above for L1, and was obtained as light yellow powder. Yield, (73%). ^{1}H NMR (400 MHz, $CDCl_3$ δ ppm): 8.700 (d, J = 4.8 Hz, 2H, H^2), 8.634 (s, 2H, H—C═N), 8.200 (d, J = 8.0 Hz, 2H, H^5), 7.800 (t, 2H, H^4), 7.352 (t, 2H, H^3), 7.306–7.229 (m, 8H, $H^{a,b}$), 7.150 (s, 4H, H^c), 1.694 (s, 12H, CH_3); IR (KBr cm^{-1}): v = 3055 (w), 2962 (m), 2927 (w), 1630 (m), 1564 (w), 1504 (vs), 1469 (m), 1389 (w), 1207 (w), 1090 (w), 1016 (w), 883 (m), 838 (s), 779 (m); Anal. Calcd (%) for $C_{36}N_4H_{34}$: C 82.72, H 6.56, N 10.72, Found: C 82.79, H 6.50, N 10.71.

*Synthesis of $[Ni_2(L1)_3][ClO_4]_4$ (**1**)*

To a stirred suspension of ligand L1 (0.09 mmol, 0.042 g) in 10 mL acetonitrile, a MeCN solution (10 mL) of $Ni(ClO_4)_2$ $6H_2O$ (0.06 mmol, 0.022 g) was added dropwise. The resultant orange mixture was heated at reflux temperature for 5 h and allowed to cool. The resulting orange solution was filtered through Celite and the filtrate was evaporated to dryness under reduced pressure. The residue was dissolved in 10 mL MeCN from which orange microcrystalline powder was retrieved by filtration after a few days following the slow diffusion of ether into the MeCN solution. Yield, (44%). ESI-MS (m/z): 382.33 $[Ni_2(L1)_3]^{4+}$ 100%, 542.75 $[Ni_2(L1)_3(ClO_4)]^{3+}$ 30%, 863.25 $[Ni_2(L1)_3(ClO_4)_2]^{2+}$ 23%; IR (KBr cm^{-1}): V = 3070 (w), 1631 (w), 1593 (s), 1497 (vs), 1477 (w), 1444 (w), 1263 (w), 1223 (w), 1078 (vs), 968 (w), 845 (m), 777 (w), 623 (m); UV–Vis (H_2O/MeCN nm): 331 (ε = 15150), 282 (ε = 23000), 241 (ε = 37500), 205 (ε = 77600); Anal. Calcd (%) for $Ni_2C_{90}N_{12}O_{22}H_{66}Cl_4$: C 56.10, H 3.45, N 8.72, Found: C 56.21, N 8.67, H 3.51.

*Synthesis of $[Ni_2(L2)_3][ClO_4]_4$ (**2**)*

$[Ni_2(L2)_3][ClO_4]_4$ (**2**) was prepared by the same method as above for **1** but with ligand L2 (0.09 mmol, 0.047 g) to give a yield of 40%. ESI-MS (m/z): 421.42 $[Ni_2(L2)_3]^{4+}$ 93%, 594.83 $[Ni_2(L2)_3(ClO_4)]^{3+}$ 100%, 941.42 $[Ni_2(L2)_3(ClO_4)_2]^{2+}$ 67%; IR (KBr cm^{-1}): V = 3057 (w), 2972 (w), 2870 (w), 1624 (w), 1599 (w), 1541 (w), 1504 (w), 1451 (w), 1361 (w), 1117 (vs), 1086 (s), 841 (w), 777 (w), 629 (m); UV–Vis (H_2O/MeCN nm): 329 (ε = 18,700), 245 (ε = 25,500), 205 (ε = 81,050); Anal. Calcd (%) for $Ni_2C_{108}N_{12}O_{16}H_{102}Cl_4$: C 62.27, H 4.93, N 8.07, Found: C 62.33, H 4.89, N 8.10.

*Synthesis of $[Ni_2(L3)_3][ClO_4]_4$ (**3**)*

$[Ni_2(L3)_3][ClO_4]_4$ (**3**) was prepared by the same method as above for **1** but with ligand L3 (0.09 mmol, 0.047 g) to give a yield of 35%. ESI-MS (m/z): 421.42 $[Ni_2(L3)_3]^{4+}$ 100%, 594.92 $[Ni_2(L3)_3(ClO_4)]^{3+}$ 71%, 941.25 $[Ni_2(L3)_3(ClO_4)_2]^{2+}$ 17%; IR (KBr cm^{-1}): v = 3070 (w), 2968 (w), 2887 (w), 1629 (w), 1597 (w), 1500 (w), 1363 (w), 1261 (w), 1086 (s), 1020 (w), 802 (m), 625 (m); UV–Vis (H_2O/MeCN nm): 338 (ε = 18,750), 247 (ε = 31,250), 205 (ε = 75,000); Anal. Calcd (%) for $Ni_2C_{108}N_{12}O_{16}H_{102}Cl_4$: C 62.27, H 4.93, N 8.07, Found: C 62.32, H 4.97, N 8.12.

Molecular mechanics modelling studies

Molecular mechanics calculations on $[Ni_2(L1)_3]^{4+}$, $[Ni_2(L2)_3]^{4+}$ and $[Ni_2(L3)_3]^{4+}$ were carried out with Hyperchem Version 7.52 [19]. The modelling studies were limited to use MM+ with the Polak-Ribiere algorithm of Hyperchem and the energy minimized at an RMS gradient of 0.01. Molecular dynamics was also used (simulated heating to 3000 K) to make sure the true energy minima had been reached. The original *rac*- and *meso*-configurations of complexes **1–3** were arranged roughly by eye and guided by the ESI-MS, UV–Vis and IR spectroscopic data.

DNA-binding studies

Absorption spectroscopy

To determine the binding affinity of the complexes **1–3** with HTG22 and ct-DNA, the complexes (4–20 μM) were titrated with DNA solutions (HTG22 in buffer B: from 0 to 1.26 μM, and ct-DNA in buffer D: from 0 to 200 μM). The same volume of DNA solution was added to each cuvette to eliminate the absorbance of DNA itself, and the solutions were mixed by repeated inversion. A buffer solution baseline was subtracted from each data set. After mixing for 5 min, the absorption spectra were recorded. The changes in the metal complex concentration due to dilution at the end of each titration were negligible. The UV–Vis titrations for each sample were repeated at least three times.

Circular dichroism spectroscopy

Circular dichroism (CD) titrations were carried out using a MOS-450/AF-CD spectropolarimeter at room temperature with fixed concentration constant at 2 μM of HTG22 DNA. By adding the solutions of metal complex to the 0.5 cm pathlength cell, the HTG22 DNA:metal complex ratios were 2:1, 1:1, 2:3, 2:4 and 2:6, respectively. All solutions were mixed thoroughly and allowed to equilibrate for 5 min before data collection. For each sample, the

spectrum was scanned at least three times and accumulated over the wavelength range. The instrument was flushed continuously with pure evaporated nitrogen throughout the experiment. The scan of the buffer alone was subtracted from the average scan for each sample.

Fluorescence resonance energy transfer (FRET) studies

The fluorescent-labeled oligonucleotide, F22T, used as the FRET probes were diluted in buffer B solution and annealed after heating to 95 °C for 5 min, and then incubated at 4 °C overnight. Fluorescence melting curves were determined by using a Bio-Rad iQ5 real-time PCR detection system. Different concentrations of complexes were added into a total reaction volume of 20 μL with 0.2 μM of labeled oligonucleotide. Fluorescence readings with excitation were taken at intervals of 1 °C over the range 20–90 °C, with a constant temperature being maintained for 30 s prior to each reading to ensure a stable value. The melting of the G-quadruplex was monitored alone or in the presence of various concentrations of complexes. Various concentrations of competitors (double stranded self-complementary ds26 DNA) were added to test the binding selectivity of the compound to the quadruplex structure. Final analysis of the data was carried out using Origin 7.5 software (Origin Lab Corp.).

Results and discussion

Synthesis and characterization

The dinuclear triple-stranded cylinders **1–3** were prepared by reactions of $Ni(ClO_4)_2$ with the tetradentate ligands L1, L2 and L3, respectively. The ligands and complexes were characterized by various spectroscopic and analytical techniques. In the ^1H NMR spectra of the ligands L1–L3 (Fig. S1), H—C═N protons showed singlet at about 8.63, the protons of pyridine appeared at 8.70–7.35, and the peeks at 7.30–6.70 belonged to the protons of benzene. In the IR spectra, the characteristic peaks near 1630 cm^{-1} were assigned to the $\nu_{C=N}$ stretching vibration of the ligands. After coordinating with nickel(II) ions, the characteristic $\nu_{C=N}$ peaks shifted to lower wave numbers. Meanwhile, the peeks at 1088 cm^{-1} and 630 cm^{-1} revealed the existence of ClO_4^-, which confirmed metal center involvement in bis(pyridylimine) Schiff base units. UV–Vis spectra observed from 200 to 300 nm for **1–3** were due to in-ligand (IL) transitions, while the peaks around 330 nm were characteristic metal → ligand charge transfer (MLCT) transitions for nickle(II) complexes. The ESI-MS of complexes **1–3** in acetonitrile-methanol solution revealed the presence of molecular ion peaks $[Ni_2(L1)_3]^{4+}$, $[Ni_2(L2)_3]^{4+}$ and $[Ni_2(L3)_3]^{4+}$ with varying numbers of associated ClO_4^- (Fig. S2). For example, the peaks of complex **1** at *m*/*z* 382, 542 and 863 corresponded to $[(Ni_2(L1)_3)(ClO_4)_n]^{(4-n)+}$ (n = 0, 1, 2), indicating that $Ni_2(L1)_3^{4+}$ is the most stable fragment in solution. The peak values of the great abundant fragment ions observed in ESI-MS spectra for complexes **1–3** were in agreement with the calculated values (Table S1). From the above, three new dinuclear nickel(II) triple-stranded supramolecular cylinders have been synthesized successfully.

Molecular mechanics modelling studies

To further confirm the structures of the Ni(II) Schiff base complexes **1–3**, the molecular simulate modelling studies were performed. The compounds we used, all have bimetallo triple-stranded structures, in which two configurations are possible: a *rac* isomer (the isomer is chiral and is one of a pair of enantiomers) and a *meso* isomer rendering the structure achiral [20]. According to the lowest energy principle, the energy of the cylinders **1–3** was minimized to 173.13, 181.69 and 183.46 kcal mol^{-1}, which corresponded to the structure of *meso*-$[Ni_2(L1)_3]^{4+}$, *rac*-$[Ni_2(L2)_3]^{4+}$ and *rac*-$[Ni_2(L3)_3]^{4+}$, respectively (Fig. 1). Complex **1** mainly exists in *meso*-configuration, while complexes **2** and **3** mainly exist in *rac*-configuration. As listed in Table 1, the sizes of cylinders **1–3** were found slight larger than the traditional nickel(II) cylinder $Ni_2(L)_3^{4+}$ (length ~ 18 Å, width ~ 8 Å) [21]. The cylinder **1** containing 1,3-bisphenoxylbenzene spacers is longer and narrower than **2** and **3**, because the O linked bridging ligand L1 is more rigid than L2 and L3 formed $CH(CH_3)_2$ bind and cannot spiral easily. However, **2** and **3** with *rac*-configuration have larger intracavities than **1** with *meso*-configuration. The structural simulation information of complexes **1–3** was favorable to explain their different DNA binding features.

DNA binding experiments

Electronic absorption spectroscopy

UV–Vis spectrum was performed to determine the binding affinities for complexes **1–3** toward quadruplex (HTG22) and duplex DNA (ct-DNA). As the successive addition of HTG22 to the solution of complexes **1–3**, both intraligand absorption band from 200 to 300 nm and metal → ligand charge transfer (MLCT) at about 330 nm displayed significantly hypochromism (*H*%), indicating the strong interaction between the dinuclear triple-stranded cylinders and G-quadruplex DNA bases (Fig. 2). In general, the extent of hypochromism parallels the DNA-binding strength of the complex [22]. As addition of 1.26 μM HTG22 to 4 μM complexes **1**, **2** and **3,** the band at 205 nm exhibited the max hypochromism of 34.7%, 29.9% and 19.4%, respectively. This indicated that the complex **1** bound more tightly to G-quadruplexes than complexes **2** and **3** did. In contrast, as the ratio of [ct-DNA]/[complex] increased to 10, all three complexes demonstrated large hypochromicity

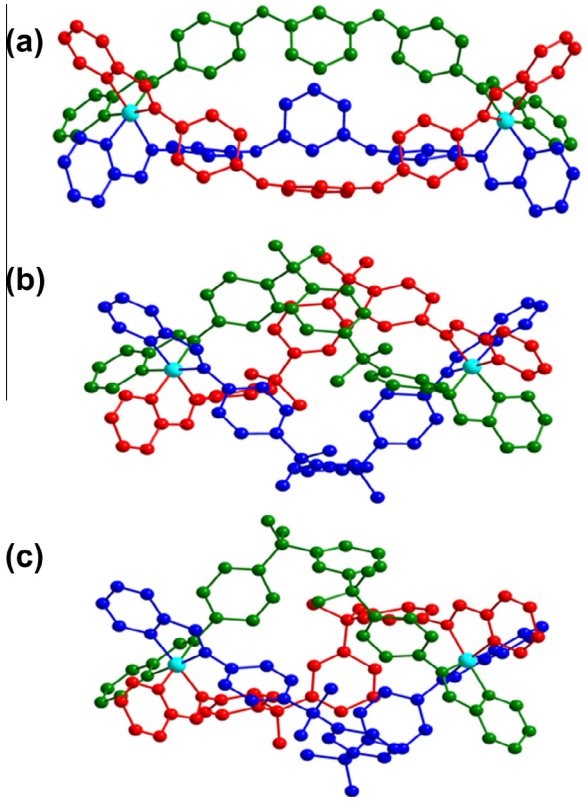

Fig. 1. The molecular models of tetracationic triple-stranded supramolecular cylinders: (a) $[Ni_2(L1)_3]^{4+}$, (b) $[Ni_2(L2)_3]^{4+}$, and (c) $[Ni_2(L3)_3]^{4+}$.

Table 1
Structural simulation data of complexes **1**–**3**.

Complex	Configuration	Energy (kcal mol^{-1})	Length (Å)	Diameter (Å)
1	*rac-*	177.14	22.38	9.42
	meso-	173.13	22.67	9.00
2	*rac-*	181.69	19.69	13.43
	meso-	193.28	23.37	12.47
3	*rac-*	183.46	19.26	14.86
	meso-	190.59	22.73	13.41

(>30%) at 205 nm suggesting **1**–**3** could also bind to duplex ct-DNA (Fig. S3).

In order to compare quantitatively the binding strength of **1**–**3** to G4-DNA and ct-DNA, the intrinsic binding constants K_b with DNA were obtained using the following equation [23]:

$$[D]/\Delta\varepsilon_{ap} = [D]/\Delta\varepsilon + 1/(K_b \times \Delta\varepsilon), \quad \Delta\varepsilon_{ap} = |\varepsilon_a - \varepsilon_f|, \quad \Delta\varepsilon = |\varepsilon_b - \varepsilon_f|$$

where $[D]$ is the concentration of DNA in base pair, ε_a, ε_b and ε_f are the apparent extinction coefficient (A_{obs}/[complex]) and the extinction coefficient for nickle(II) complex in the free and fully bound form, respectively. K_b is the equilibrium binding constant in M^{-1}. As listed in Table 2, the G4-DNA binding constants of **1–3** were comparable to that of other compounds reported to be good G-quadruplex DNA binders (10^6 M^{-1} range) [24]. Moreover, complexes **1–3** displayed reasonable selectivity (ca. 2 orders of magnitude) for quadruplex versus duplex DNA. The trend of G4-DNA binding constant $^{G4\text{-}DNA}K_b$ was **1** > **2** > **3** which was consistent with the order of hypochromicity. However, when bound to ct-DNA, the $^{ct\text{-}DNA}K_b$ order was **3** > **2** > **1**. The different binding affinities to quadruplex and duplex DNA of **1–3** could be attributed to the structural differentiation.

Circular dichroism spectroscopy

Circular dichroism (CD) spectroscopy is uniquely sensitive to the absorption of the solution conformations of HTG22. Without any metal cations in HTG22 solution, the DNA molecules not only exist as a mixture of parallel and antiparallel G-quadruplex conformations, but also are dissociated partially to single-stranded molecules [25]. With the addition of complex **1** to HTG22 aqueous solution, the distinct spectral changes that the intensity of the positive CD band at 256 nm decreased gradually from positive to negative, and a remarkable increase of the CD band at 290 nm were observed. (Fig. 3a-1) This induced CD spectrum suggested complex **1** could fold single-stranded human telomeric DNA to form a hybrid G-quadruplex structure under salt deficient conditions. However, addition of 1–10 μM **2** or **3** to HTG22 DNA in the absence of metal ions solution, the positive CD band at 256 nm decreased gradually but the peak close to 290 nm initially increased and then slowly declined when the added complex was more than 6 μM

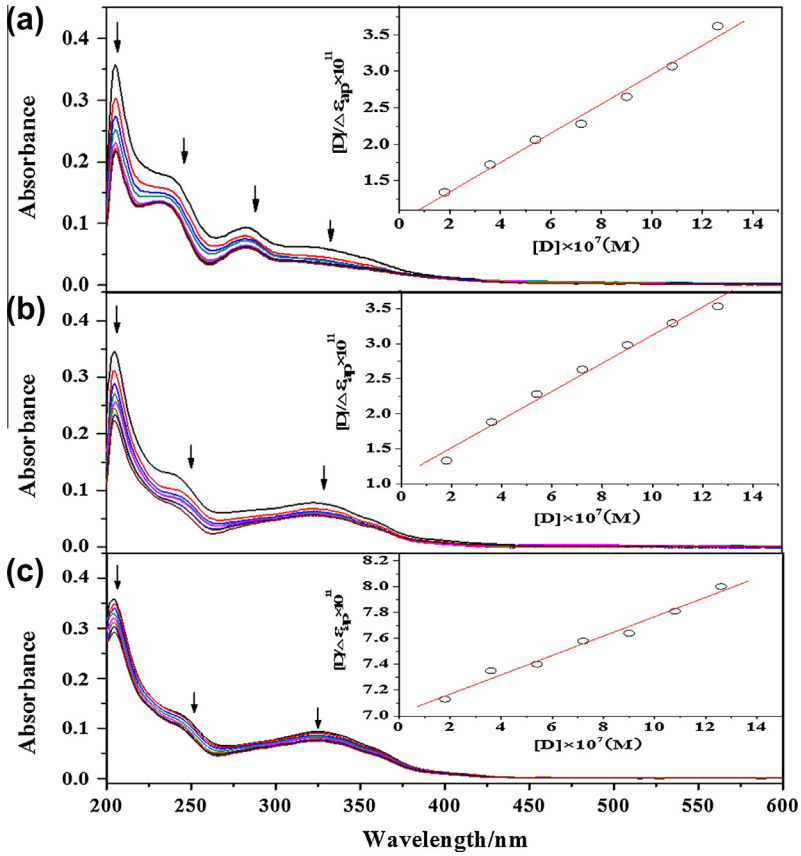

Fig. 2. UV–Vis spectra of complexes: (a) **1**, (b) **2** and (c) **3** (4 μM) in buffer B with HTG22 (0–1.26 μM). The arrows indicate the change upon increasing amount of HTG22 added. Inset: plot of $[D]/\triangle\varepsilon_{ap}$ versus [D].

Table 2
Absorption spectra (λ_{max}/nm) and DNA-binding data of complexes **1**–**3**.

Complexes	λ_{max}(free) (nm)	H (%)	$^{G4\text{-}DNA}K_b$ (M^{-1})	$^{ct\text{-}DNA}K_b$ (M^{-1})
1	331	21.6		
	282	25.3		
	241	19.6		
	205	34.7	2.2×10^6	4.0×10^3
2	329	18.4		
	245	22.6		
	205	29.9	2.0×10^6	2.0×10^4
3	338	12.6		
	247	22.9		
	205	19.4	1.1×10^5	2.3×10^4

(Fig. 3a-2 and a-3). The latter suggested that complexes **2** and **3** were able to interact with the single-strand human telomeric DNA and partially induced it to form G-quadruplex structures.

The structures of G-quadruplexes were also investigated in the Na^+ or K^+ buffer solution. Previous studies showed that human telomeric G-quadruplex could form an antiparallel structure in the presence of sodium or adopt a hybrid structure in the presence of potassium [26,27]. With addition of complex **1** to HTG22 in Na^+ buffer solution, major positive CD band significantly increased and shifted from 295 to 290 nm, accompanied by a sharp decrease around 260 and 245 nm with band shift. (Fig. 3b-1). The induced CD spectra produced by complex **1** was similar to the findings of $[Ni_2L_3]^{4+}$ complex [12]. Moreover, after addition of complex **1** to HTG22 in K^+ buffer solution, no significant change in CD spectra was found (Fig. 3c-1). These results indicated that complex **1** could convert the antiparallel G-quadruplex into a hybrid-type G-quadruplex in Na^+ solution and stabilize the hybrid G-quadruplex structure in K^+ solution. However, adding complexes **2** or **3** to HTG22 in Na^+ (Fig. 3b-2 and b-3) or K^+ (Fig. 3c-2 and c-3) buffer solution, the CD spectra exhibited a maxima-minima pattern, similar but not identical to the original spectra without addition of the complex. These CD phenomena of **2** and **3** were consistent with the reported η^6-arene ruthenium complexes [28]. Similar conclusions were drawn that complexes **2** and **3** disturbed DNA structure slightly and the DNA secondary structure did not change even at high ionic strength. The above CD studies clearly demonstrated that **1** bound to G4-DNA more strongly than complexes **2** and **3**, and only cylinder **1** of the three complexes could lead to the conversion of antiparallel G-quadruplexes to hybrid G-quadruplexes. To the best of our knowledge, a very high level CD signal conversion is rare among the molecules as G-quadruplexes stabilizers [12].

Thermodynamic stabilization of the telomeric G-quadruplex by complexes

Fluorescence resonance energy transfer (FRET) was used as a convenient method to provide information on the folded or

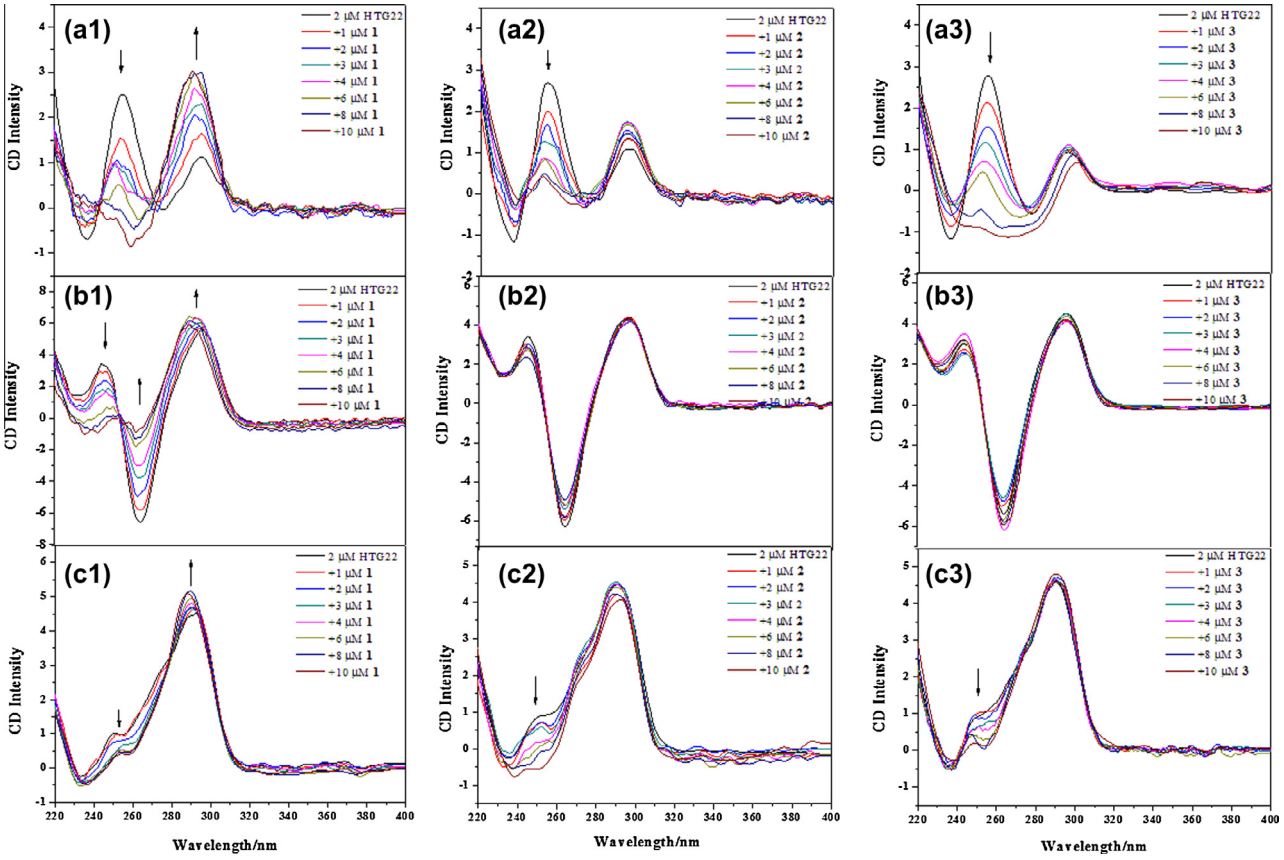

Fig. 3. CD titration spectra of HTG22 (2 μM) induced by the three compounds (from left to right: **1**, **2** and **3**) in 10 mM Tris–HCl, pH 7.4, at room temperature. (a) In the absence of metal ions, (b) in 100 mM NaCl, and (c) in 100 mM KCl.

unfolded state of the quadruplex by monitoring the 3′- to -5′ end distance [29]. The effect on the thermal stabilities of the cylinders **1**–**3** upon adding G4-DNA was explored by UV–Vis absorbance at 205 nm. The results (Fig. S4) showed that all cylinders **1**–**3** were stabilized in the presence of the G4-DNA at high temperature. We performed the FRET melting assay to investigate thermodynamic stability of complexes **1–3** to G-quadruplex DNA F22T (sequence: FAM-AG3(T2AG3)3-TAMRA, mimicking the human telomeric repeat). As shown in Fig. 4a–c, all the three complexes **1–3** significantly increased the melting temperature of the F22T with [complex]/[DNA] ratios = 1:2, 1.25:1, 2.5:1, 3.75:1 and 5:1, while ligands L1–L3 had no effect on G4-DNA with $\Delta T_m \approx 0$ °C (Fig. S5). At the ratio of 5, complex **1** induced a high degree of stabilization for G-quadruplex DNA, as demonstrated by an increase in melting temperature (ΔT_m) of 24.5 °C (Fig. 4d). Compared with **1**, complexes **2** and **3** (ΔT_m = 17.3 °C and 10.8 °C respectively) were less effective G-quadruplex DNA stabilizers, which was consistent with UV and CD studies. Moreover, the FRET-melting data confirmed that **1–3** were better G-quadruplexes binders than the chiral nickel(II) cylinder *P*-$Ni_2L_3^{4+}$ (ΔT_m = 10.6 °C) [12]. The changes in size of the cylinders **1–3** might afford larger molecular surfaces which were favorable for the stacking through the extensive hydrophobic exterior of the cylinders on the top face of the G-quadruplexes. Nevertheless, the ΔT_m values for cylinders **1–3** were lower than the reported planar nickel(II) salphen complexes (ΔT_m = 33.2 °C) [10]. This was probably because the planar arrangement of the salphen rings was able to interact with the G-quadruplexes through strong π-π stacking.

A competition FRET experiment of the telomeric sequence F22T versus non-fluorescent duplex DNA (ds26) was assessed to further determine the G-quadruplexes selectivity of cylinders **1–3** (Fig. 5). The competition FRET experiment was processed by maintaining the concentration of complex (1.0 μM) and F22T (0.2 μM) as constant with varying the ratio of [ds26]:[F22T] from 0 to 50. With the [ds26]:[F22T] ratio of 10, the thermal stabilization of F22T enhanced by **1–3** was slightly affected. Even at the addition of a 50-fold excess of ds26 DNA, the enough high ΔT_m values of F22T for **1–3** were still observed in Fig. 5d. This means that complexes **1–3** can stabilize the G-quadruplex even with the addition of substantial amounts of competitive ds26 DNA. The results of FRET competition assay demonstrated that complexes **1–3** can be considered as a new class of G-quadruplex DNA binders, and **1** was found to have stronger preference for binding to the G-quadruplex over duplex DNA than **2** or **3** did. However, the selectivity (at least 10-fold) of G-quadruplex versus duplex DNA for complexes **1–3** was lower than that of nickel salphen complexes with cyclic amine side arms (50-fold) [10]. It's probable that such cylinders with proper width and length are suitable for the configuration of the major groove of duplex DNA helix and have a bending effect on duplex DNA [30].

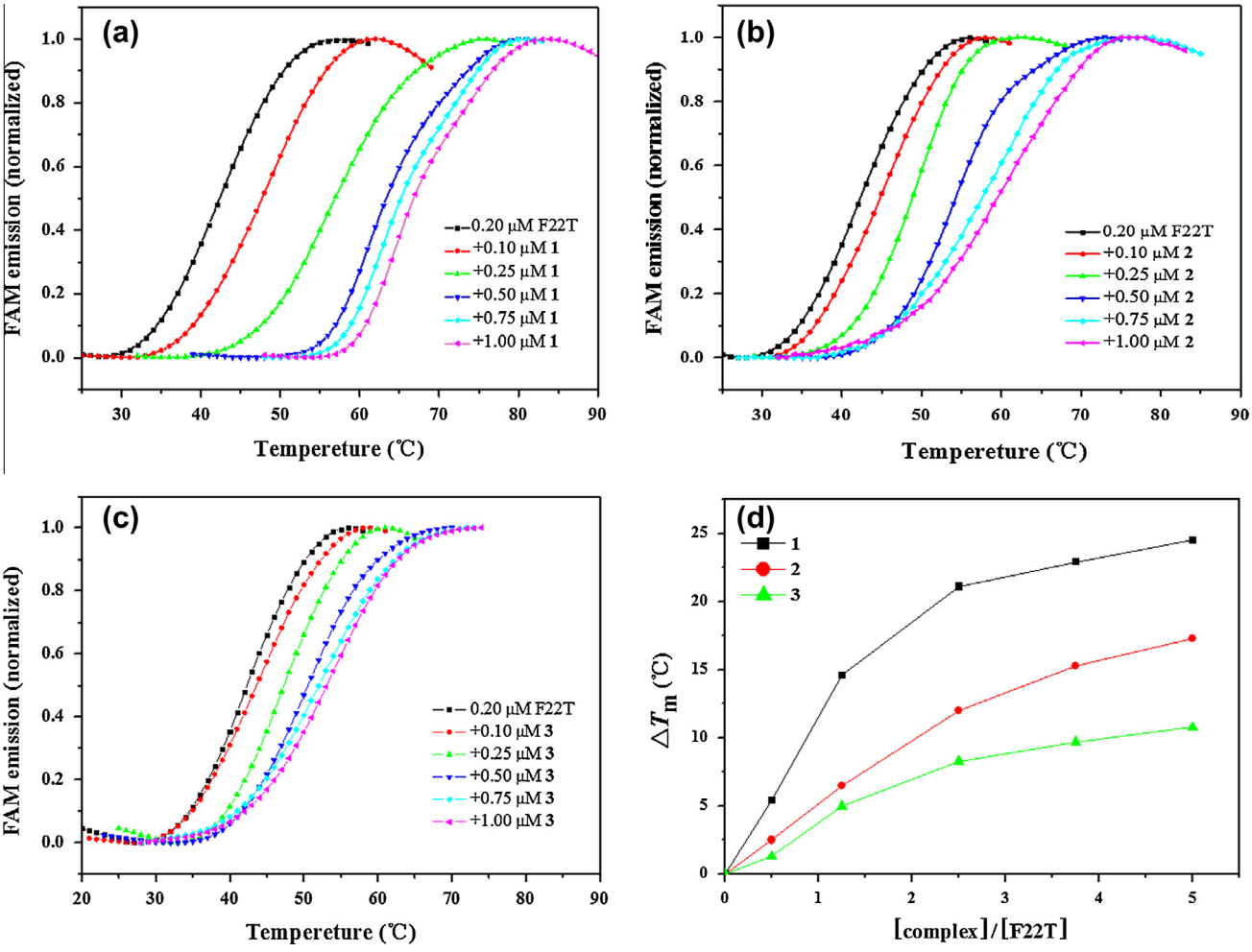

Fig. 4. FRET melting curves for experiments carried out with F22T alone and separately with (a) **1**, (b) **2** and (c) **3**. F22T concentration was 0.2 μM in Buffer B. (d) Plot of DNA stabilization temperature versus the concentration of **1** (black), **2** (red) and **3** (green) binding to F22T. (For interpretation of the references to color in this figure legend, the reader is referred to the web version of this article.)

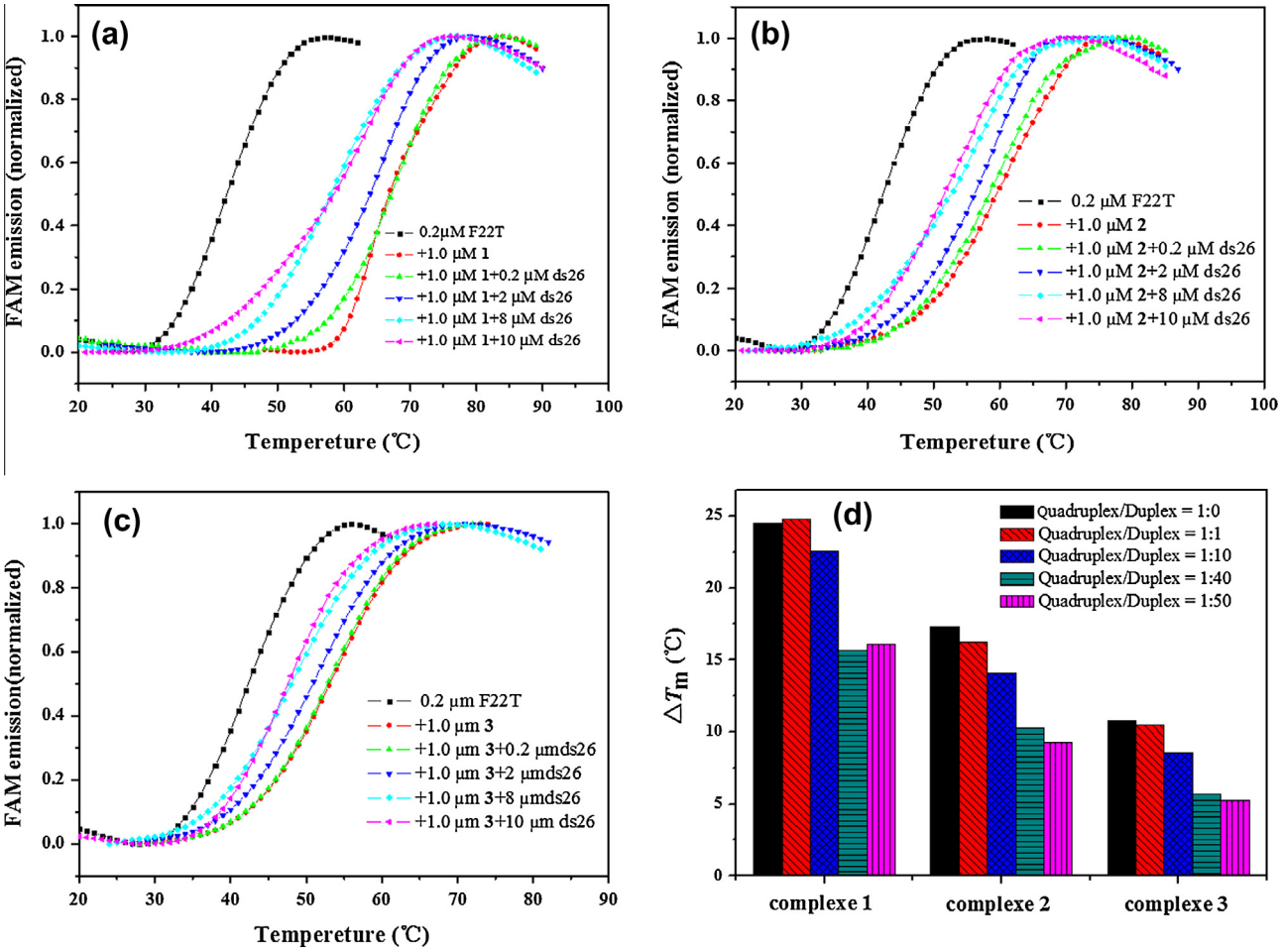

Fig. 5. Competitive FRET melting curves of F22T (0.2 μm) with 1.0 μm of (a) **1**, (b) **2**, (c) **3** and duplex competitor ds26 in Buffer B. (d) Competition FRET experiment of complexes for the G-quadruplex DNA sequence over duplex DNA. Results are the mean values of at least three independent experiments.

Possible G4-DNA binding behavior

The sizes of synthetic dinuclear nickel(II) triple-stranded supramolecular cylinders **1–3** were calculated by molecular mechanics modelling studies (Table 1), which were compatible with G-quartet (length ~ 14 Å, width ~ 11 Å). From the point of view of structures, it is difficult for cylinders **1–3** to be embedded in a π-stacking unit to the G-tetrads. Combining with UV and CD spectra studies, we can speculate that the charged cylinder is most likely as a whole to stack on the tail of G-quadruplexes. Such end-stacking model of compounds onto the G-quartet is in agreement with the previous reported cylindrical quadruplex binders [12,13]. The precise size and shape of the cylinders are crucial to determine such binding sites and modes to G-quadruplexes. In addition, four positive charges schlepped by cylinders **1–3** enhance the electrostatic interactions between the metal complex fragment and DNA's phosphate backbone. Moreover, the large hydrophobic exterior of **1–3** may also enhance the non-covalent interactions between the complexes and grooves or loops of quadruplexes. The details of the binding modes are not clear yet and deserve further investigation. Fig. 6 is the representative illustration of a proposed model of complex **1** binding to human telomeric DNA (PDB code 1KF1). It is the largest length (~22 Å) and suitable width (~9 Å) in the three cylinders that lead complex **1** to stacking most strongly on the top of a terminal G-quartet. However, the larger width (~14 Å) of complexes **2** and **3** slightly exceed the recognition surface of G-quadruplex DNA (width ~ 11 Å) and this may reduce the binding affinity of **2** and **3** to G-quartet. This is consistent with the conclusion of experiential results that complex **1** has the most excellent binding affinity to G-quadruplexes in the three complexes.

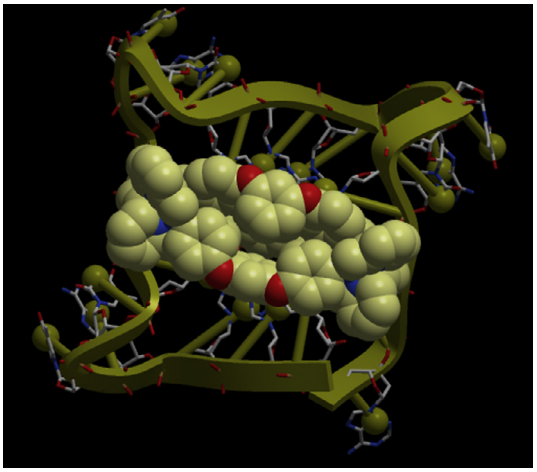

Fig. 6. Predicted interaction between **1** (shown as a ball model) and the intermolecular G-quadruplex (shown as a stick model).

Conclusion

In summary, three dinuclear nickel(II) triple-stranded supramolecular cylinders **1–3** with different bis(pyridylimine) Schiff base ligands have been successfully prepared to study their

G-quadruplexes binding properties. The three novel nickel(II) cylinders were good G-quadruplex DNA stabilizers and showed different features on DNA binding affinity. The suitable size and four positive charges of the complexes are the major factors determining the high efficiency of binding G4-DNA. Such supramolecular cylinders definitely represent a new and exciting strategy on designing new antitumor agents for targeting quadruplexes DNA. Other novel supramolecular metallaclusters as G-quadruplexes inducers and stabilizers are currently being investigated in our laboratory.

Acknowledgements

This work was supported by the National Natural Science Foundation of China (21101078 and 21276105), the Program for New Century Excellent Talents in University of China (NCET-11-0657), the Natural Science Foundation of Jiangsu Province (BK2011143), the Fundamental Research Funds for the Central Universities (JUSRP51314B), and the Ministry of Education and the State Administration of Foreign Experts Affairs for the 111 Project (B13025).

Appendix A. Supplementary material

Supplementary data associated with this article can be found, in the online version, at http://dx.doi.org/10.1016/j.saa.2013.12.102.

References

[1] (a) J.T. Davis, Angew. Chem. Int. Ed. 43 (2004) 668–698;
(b) H.Z. He, D.S.H. Chan, C.H. Leung, D.L. Ma, Nucleic Acids Res. 41 (2013) 4345–4359.
[2] (a) S. Burge, G.N. Parkinson, P. Hazel, A.K. Todd, S. Neidle, Nucleic Acids Res. 34 (2006) 5402–5415;
(b) O. Doluca, J.M. Withers, V.V. Filichev, Chem. Rev. 113 (2013) 3044–3083.
[3] P. Murat, Y. Singh, E. Defrancq, Chem. Soc. Rev. 40 (2011) 5293–5307.
[4] (a) W.D. Wilson, H. Sugiyama, ACS Chem. Biol. 2 (2007) 589–594;
(b) D.S. Pilch, C.M. Barbieri, S.G. Rzuczek, E.J. Lavoie, J.E. Rice, Biochimie 90 (2008) 1233–1249.
[5] (a) S. Balasubramanian, S. Neidle, Curr. Opin. Chem. Biol. 13 (2009) 345–353;
(b) A. De Cian, L. Lacroix, C. Douarre, N. Temime-Smaali, C. Trentesaux, J.-F. Riou, J.-L. Mergny, Biochimie 90 (2008) 131–155.
[6] T.M. Ou, Y.J. Lu, J.H. Tan, Z.S. Huang, K.Y. Wong, L.Q. Gu, Chem. Med. Chem. 3 (2008) 690–713.
[7] (a) A.K. Jissy, A. Datta, ChemPhysChem 13 (2012) 4163–4172;
(b) A.K. Jissy, U.P.M. Ashik, A. Datta, J. Phys. Chem. C 115 (2011) 12530–12536.
[8] (a) A. Arola, R. Vilar, Curr. Top. Med. Chem. 8 (2008) 1405–1415;
(b) D. Monchaud, M.-P. Teulade-Fichou, Org. Biomol. Chem. 6 (2008) 627–636;
(c) M. Micco, G.W. Collie, A.G. Dale, S.A. Ohnmacht, I. Pazitna, M. Gunaratnam, A.P. Reszka, S. Neidle, J. Med. Chem. 56 (2013) 2959–2974.
[9] (a) D.P.N. Gonçalves, R. Rodriguez, S. Balasubramanian, J.K.M. Sanders, Chem. Commun. 45 (2006) 4685–4687;
(b) S.N. Georgiades, N.H. Abd Karim, K. Suntharalingam, R. Vilar, Angew. Chem. Int. Ed. 49 (2010) 4020–4034.
[10] (a) J.E. Reed, A.A. Arnal, S. Neidle, R. Vilar, J. Am. Chem. Soc. 128 (2006) 5992–5993;
(b) A.A. Arnal, J. Benet-Buchholz, S. Neidle, R. Vilar, Inorg. Chem. 47 (2008) 11910–11919.
[11] (a) R. Kieltyka, P. Englebienne, J. Fakhoury, C. Autexier, N. Moitessier, H.F. Sleiman, J. Am. Chem. Soc. 130 (2008) 10040–10041;
(b) S. Shi, J. Liu, T. Yao, X. Geng, L. Jiang, Q. Yang, L. Cheng, L. Ji, Inorg. Chem. 47 (2008) 2910–2912;
(c) Y.-L. Wu, K.E. Brown, M.R. Wasielewski, J. Am. Chem. Soc. 135 (2013) 13322–13325.
[12] H.J. Yu, X.H. Wang, M.L. Fu, J.S. Ren, X.G. Qu, Nucleic Acids Res. 36 (2008) 5695–5703.
[13] C.Q. Zhao, J. Geng, L.Y. Feng, J.S. Ren, X.G. Qu, Chem. Eur. J. 17 (2011) 8209–8215.
[14] (a) M.J. Maroney, Curr. Opin. Chem. Biol. 3 (1999) 188–199;
(b) P.E. Carrington, P.T. Chivers, F. Al-Mjeni, R.T. Sauer, M.J. Maroney, Nat. Struct. Biol. 10 (2003) 126–130.
[15] (a) S. Sarkar, A. Datta, A. Mondal, D. Chopra, J. Ribas, K.K. Rajak, S.M. Sairam, S.K. Pati, J. Phys. Chem. B110 (2006) 12–15;
(b) N.S. John, G.U. Kulkarni, A. Datta, S.K. Pati, F. Komori, G. Kavitha, C. Narayana, M.K. Sanyal, J. Phys. Chem. C 111 (2007) 1868–1870;
(c) A. Datta, N.S. John, G.U. Kulkarni, S.K. Pati, J. Phys. Chem. A 109 (2005) 11647–11649.
[16] X.D. Dong, X.Y. Wang, Y.F. He, Z. Yu, M.X. Lin, C.L. Zhang, J. Wang, Y.J. Song, Y.M. Zhang, Z.P. Liu, Y.Z. Li, Z.J. Guo, Chem. Eur. J. 16 (2010) 14181–14189.
[17] M.E. Reichmann, S.A. Rice, C.A. Thomas, P. Doty, J. Am. Chem. Soc. 76 (1954) 3047–3053.
[18] J. Marmur, P. Doty, J. Mol. Biol. 3 (1961) 585–594.
[19] S. Goetz, P.E. Kruger, Dalton Trans. 35 (2006) 1277–1284.
[20] C. Uerpmann, J. Malina, M. Pascu, G.J. Clarkson, V. Moreno, A. Rodger, A. Grandas, M.J. Hannon, Chem. Eur. J. 11 (2005) 1750–1756.
[21] (a) L.J. Childs, M.J. Hannon, Supramol. Chem. 16 (2004) 7–22;
(b) M.J. Hannon, I. Meistermann, C.J. Isaac, C. Blomme, J. Aldrich-Wright, A. Rodger, Chem. Commun. (2001) 1078–1079.
[22] C. Wei, G. Jia, J. Yuan, Z. Feng, C. Li, Biochemistry 45 (2006) 6681–6691.
[23] A. Wolfe, G.H. Shimer Jr., T. Meehan, Biochemistry 26 (1987) 6392–6396.
[24] (a) R. Kieltyka, J. Fakhoury, N. Moitessier, H.F. Sleiman, Chem. Eur. J. 14 (2008) 1145–1154;
(b) K. Suntharalingam, A.J.P. White, R. Vilar, Inorg. Chem. 49 (2010) 8371–8380.
[25] Y. Xu, Y. Noguchi, H. Sugiyama, Bioorg. Med. Chem. 14 (2006) 5584–5591.
[26] J.S. Ren, X.G. Qu, J.O. Trent, J.B. Chaires, Nucleic Acids Res. 30 (2002) 2307–2315.
[27] J. Dai, M. Carver, C. Punchihewa, R.A. Jones, D. Yang, Nucleic Acids Res. 35 (2007) 4927–4940.
[28] D.D. Sun, R. Zhang, F. Yuan, D. Liu, Y.H. Zhou, J. Liu, Dalton Trans. 41 (2012) 1734–1741.
[29] G.W. Collie, G.N. Parkinson, Chem. Soc. Rev. 40 (2011) 5867–5892.
[30] M.J. Hannon, Chem. Soc. Rev. 36 (2007) 280–295.